ELSEVIER

Global and Planetary Change 9 (1994) 197–219

GLOBAL AND PLANETARY CHANGE

Joint investigations of the middle Pliocene climate II: GISS GCM Northern Hemisphere results

Mark Chandler [a], David Rind [b], Robert Thompson [c]

[a] *Columbia University, and the Goddard Institute for Space Studies, 2880 Broadway, New York, NY 10025, USA*
[b] *NASA-Goddard Space Flight Center, Institute for Space Studies, 2880 Broadway, New York, NY 10025, USA*
[c] *United States Geological Survey, 919 Federal Center, Denver, CO 80225, USA*

Received 10 August 1993; accepted after revision 11 May 1994

Abstract

Marine microfaunal data and terrestrial pollen records indicate that the middle Pliocene (ca. 3 Ma) climate is the most recent period in geologic history with global temperatures nearly as warm as those predicted for the coming century. We used the GISS GCM to examine the Pliocene climate by specifying sea surface temperatures and vegetation distributions derived from U.S.G.S. data sets. The simulation resulted in 1.4°C warming, annually averaged over the Northern Hemisphere. Warming was greatest at high latitudes; consequently, the equator to pole temperature gradient decreased by 11.5°C. Surface air temperature increases were greatest in winter, as decreased snow and sea ice triggered a positive albedo feedback effect. At low latitudes, temperatures were mostly unchanged except for an anomalous 3°C cooling over eastern Africa. This anomaly is supported by palynological data and, in the simulation, was a response to the weakening of the Hadley circulation, which caused subtropical clouds and evapotranspiration rates to increase. Evaporation and precipitation rates decreased over the oceans and the appearance of negative $P-E$ anomalies might have implications for the Pliocene thermohaline circulation. The hydrological cycle intensified over the continents, where annual evaporation, rainfall, and soil moisture all increased. However, simulated summer drought conditions are not corroborated by terrestrial records, pointing to deficiencies in either the model, the boundary conditions, or the terrestrial data interpretations.

The Pliocene SST pattern implicates increased ocean heat flux as a component force behind the middle Pliocene warmth, since levels of CO_2, large enough to cause the extreme high latitude temperatures, would generate more tropical warming than is indicated by floral and faunal records. Surface energy fluxes, calculated by the GCM, indicate that an increased meridional ocean heat flux of 32% could reproduce the data-derived SST distribution, despite weakened atmospheric transports. The decreased wind stress values suggest that any increase of ocean heat transports would probably have resulted from a strengthening of the thermohaline circulation.

1. Introduction

Furthering our understanding of climate and climate model sensitivity is critical if we hope to assess future climate change. Paleoclimate experiments are routinely used as one means of determining if global climate models (GCMs) exhibit the appropriate sensitivity to varying internal and external conditions (e.g. changes in land surface properties, atmospheric trace gases, or solar radiation). Ultimately, these computer experiments rely heavily on the ability to supply and interpret paleoclimate data. The data allows modelers to assign proper boundary conditions to the GCM and it provides an independent

SSDI 0921-8181(94)00008-2

means of assessing certain climate variables, such as temperature and hydrological properties, which can then be used for comparison with GCM results.

Despite the variety of climates that have existed in the Earth's past it is unlikely that any single scenario is an exact analog of our planet's near future. Last Glacial Maximum and Holocene climate modeling studies have provided many insights into the effect of altered forcings and feedbacks (for examples see Manabe and Broccoli, 1985; Kutzbach and Guetter, 1986; Rind, 1986; Rind, 1987a). They offer abundant data and exhibit temperature changes similar in absolute value to those found in doubled-CO_2 experiments, thus they provide superb opportunities to compare the climate sensitivity of the Earth with that of a GCM (Hansen et al., 1993; Hoffert and Covey, 1992). Ancient warm climates, such as the Jurassic (Chandler et al., 1992; Moore et al., 1992; Valdes and Sellwood, 1992), Cretaceous (Barron and Washington, 1984; 1985; Barron, 1989; Barron and Peterson, 1990), and Eocene (Sloan and Barron, 1990, Sloan and Barron, 1992), also provide scenarios that help us explore the potential affects of large changes in the climate system. These climates have less available data, but they are invaluable as simulation scenarios because they present us with a view of the Earth's climate during intervals that were much warmer than today: intervals that were as warm or warmer than a climate with twice today's CO_2 level.

One such warm time period, the middle Pliocene (ca. 3 Ma), offers perhaps the most useful scenario for climatologists who are seeking to understand and improve numerical computer models for global warming studies. The middle Pliocene exhibits many characteristics which may be quite like the anticipated climate of the next century. It was significantly warmer than the present, based on estimates from marine microfauna of ocean temperatures and on palynological data (see Dowsett et al., 1994). The planet's high latitudes, in particular, were much warmer than they are today, resulting in a reduced equator to pole temperature gradient. The Isthmus of Panama was in place by this time, forming a critical geographic barrier between the Atlantic and Pacific Oceans, thus it is less likely that the altered climate was the result of unique equatorial currents (Maier-Reimer et al., 1990).

Furthermore, the similarity between Pliocene continent/ocean distributions and those of the present make comparisons with current climate "control" simulations more feasible, since direct differences can be made of the results of the two simulations. Differencing the results with a control experiment reduces the effect of certain GCM-specific biases. Finally, model-data comparisons for middle Pliocene climates appear encouraging because: (1) paleoclimate data (and sections), for both land and oceans, are abundant (relative to earlier warm periods), (2) micropaleontologically based climate interpretations are feasible due to the large number of extant genera and species, (3) the young geologic age implies that fewer alteration problems will hamper geochemical analyses, and (4) the dating of sections is more precise, thus temporal averaging is reduced and data can be more reasonably compared with equilibrium or short-term transient climate model simulations.

There is no definitive evidence that reveals the primary climate forcing lying behind the Pliocene warmth. Circumstantial evidence suggests that increased ocean heat transports may have played a more significant role in the Pliocene warming than did increases in atmospheric carbon dioxide (Rind and Chandler, 1991; Dowsett et al., 1992; Raymo and Rau, 1992). Surface conditions were certainly different from the present: vegetation distributions were altered, (Dowsett et al., 1994), sea level was at least 25 m higher than today, and the higher sea levels suggest that the Greenland and Antarctic ice sheets were smaller than at present (Haq et al., 1987; Dowsett and Cronin, 1990; Harwood, 1986). Additionally, there has been much debate about the timing and significance of uplift in the Tibetan Plateau region (Raymo et al., 1988; Ruddiman and Kutzbach, 1989; Molnar and England, 1990; Raymo and Ruddiman, 1992; Amano and Taira, 1993; Cochran, 1993); although the focus for uplift-related climate change seems to have shifted towards earlier (7–8 Ma) epochs (Rind, 1992; Molnar et al., 1993).

Despite these differences, the middle Pliocene has more similarities with our anticipated future climate than almost any other warm period in Earth history and it is, therefore, of great interest to climatologists seeking to unravel the complex processes that result in a warming of our planet. Below we detail the results of a GCM experiment that begins to explore the causes and consequences of a warmer climate

like that of the middle Pliocene. Results and analyses presented here are the first produced from an interative data-modeling project that combines ongoing research within the U.S. Geological Survey's Global Change Program and the Goddard Institute for Space Studies (GISS) Climate Modeling Program. The companion to this paper (Dowsett et al., 1994) provides a complete description of the paleoclimate data and boundary conditions that were used in these experiments.

2. Boundary conditions and experiment design

2.1. The GISS General Circulation Model

The GISS atmospheric general circulation model has nine vertical layers in the atmosphere and two in the ground. Seven of the nine atmospheric layers are in the troposphere and two are in the stratosphere (i.e. above 100 mb). The version of the GISS GCM used for the Pliocene experiment has an 8° × 10° horizontal resolution, uses realistic topography and has a fractional grid system; a feature that allows model calculations for both land and ocean in coastal grid boxes. The GCM solves the equations for conservation of mass, energy, momentum and moisture. The radiation routine accounts for aerosols, trace gases (e.g. CO_2, CH_4, O_3, etc.), water vapor, and clouds. Both convective and large-scale cloud cover is predicted by the model. The Pliocene experiment employed a full seasonal cycle simulation with seasonal heat storage and diurnal temperature variations. Ground hydrology and surface albedo are functions of specified vegetation types (Table 1) (Matthews, 1984). Atmospheric trace gas levels were fixed at 1958 levels (CO_2 = 315 ppm) and a modern orbital configuration was used for solar insolation calculations. A complete model description and results from the current climate control experiment are presented in Hansen et al. (1983). Comparisons with doubled-CO_2 runs refer to the experiment presented in Hansen et al. (1984) and discussed in more detail by Rind (1988) and Hansen et al. (1988).

2.2. Pliocene boundary conditions

Boundary conditions in the GISS GCM (Fig. 1) can be organized into three categories: surface properties, atmospheric constituents, and external forcings. Surface boundary conditions can be further subdivided into continental and oceanic properties. In a geologic time frame, none of these boundary conditions are fixed; however, in the GCM, such features are treated as fixed since they are not allowed to respond to the calculated climate changes during the course of the experiment. Specifying sea surface temperatures (SSTs) and sea ice distribution does, in effect, impart an implicit ocean heat transport to the GCM's ocean. However, given that SSTs are probably the best known of the various data-derived surface conditions it is useful to prescribe SSTs for initial paleoclimate experiments when the objective is to reproduce a specific climate scenario.

Table 1
Vegetation characteristics used in the GISS GCM

		Desert *	Tundra	Grass	Shrub	Woodland	Deciduous	Evergreen	Rainforest
Visual albedo (%)	winter	0.35	0.07	0.09	0.09	0.08	0.10	0.07	0.06
	spring	0.35	0.06	0.10	0.10	0.07	0.05	0.07	0.06
	summer	0.35	0.08	0.09	0.14	0.08	0.06	0.08	0.06
	autumn	0.35	0.08	0.09	0.11	0.06	0.05	0.06	0.06
Near-IR albedo (%)	winter	0.35	0.20	0.27	0.27	0.23	0.30	0.20	0.18
	spring	0.35	0.21	0.35	0.30	0.24	0.22	0.20	0.18
	summer	0.35	0.30	0.36	0.42	0.30	0.29	0.25	0.18
	autumn	0.35	0.25	0.31	0.33	0.20	0.22	0.18	0.18
Water field capacity (cm)	Layer 1	1.0	3.0	3.0	3.0	3.0	3.0	3.0	14.0
	Layer 2	1.0	20.0	20.0	30.0	30.0	45.0	45.0	45.0
Masking depth (m)		0.1	0.2	0.2	0.5	2.0	5.0	10.0	25.0
Roughness length (m)		0.005	0.01	0.01	0.018	0.32	1.0	1.0	2.0

* Desert albedo is reduced by ground wetness by a factor $(1 - 0.5\ W_1)$.

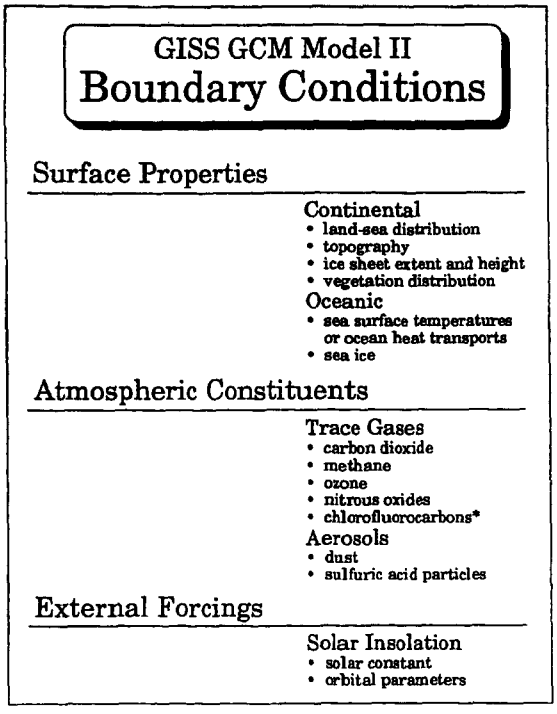

Fig. 1. Boundary conditions used in the Goddard Institute for Space Studies General Circulation Model II. Boundary conditions are the assigned physical characteristics that affect with the atmospheric circulation and/or radiative properties. They may be altered between simulations, but are fixed during the course of a simulation. Some characteristics, such as sea surface temperatures and sea ice, may be treated as boundary conditions or they can be calculated interactively by the model.

Miller et al. (1983), Russell et al. (Russell et al., 1985) and Rind and Chandler (1991) have shown that SST patterns can be reproduced with model-calculated ocean heat transports, however, such experiments are up to six times less efficient computationally. As additional forcing factors are varied in future simulations, SSTs can be given the freedom to adjust so that the full feedback potential of the oceans can be evaluated. A fully coupled ocean–atmosphere GCM would allow us to address the larger issue of impacts from the deep ocean circulation.

In the experiment described here, three boundary conditions were altered from their present day Northern Hemispheric values: SSTs, sea ice, and vegetation. The Pliocene SST and vegetation boundary conditions were reconstructed by the Pliocene Research, Interpretation, and Synoptic Mapping (PRISM) project at the U.S. Geological Survey (see Dowsett et al., 1994). Monthly sea-ice fields were generated based on the specified SST fields. Differences from modern conditions are shown in Fig. 2. For this experiment we kept Southern Hemisphere conditions at modern climatological values. PRISM data indicate that tropical and subtropical SSTs (to 25° north and south) are similar to modern values thus, low latitude conditions within both hemispheres are close to the best available estimates for the middle Pliocene. Differences between a current climate control run and the Pliocene experiment revealed that there is little interhemispheric influence, therefore, we exclude the Southern Hemisphere in our analysis. Very few data are available for the Southern Hemisphere, but there are brewing controversies regarding Southern Ocean temperatures and the size of the Antarctic ice sheet. Thus, as more information becomes available, and as data sets are compiled for use as boundary conditions, we can focus on those issues. For now, the specified SST distributions limit any dynamically or radiatively imposed effects caused by the Southern Hemisphere surface conditions and all indications are that the Northern Hemisphere results should be robust, within the limits of both the GCM parameterizations and the data interpretations.

A modern value of 315 ppm (ca. 1958) was used for the atmospheric CO_2 level, a reasonable assumption, since recent geochemical analyses and modeling studies (Rind and Chandler, 1991; Raymo and Rau, 1992) suggest that Pliocene carbon dioxide was not too far removed from its current level (± 70

Fig. 2. (a,b) February and August sea surface temperature change (°C) (Pliocene–Modern). Pliocene data were supplied by the PRISM Project members (see Dowsett et al., 1994). Monthly-average SST boundary conditions for the Pliocene GCM simulation were interpolated using a sine curve fit to the warmest (August) and coolest (February) months. (c,d) Pliocene and modern vegetation distributions. Grayscale shading shows relative albedo characteristics of vegetation types. Water field capacities of the ground layers in the GISS GCM are also determined by the assigned vegetation type (see Table 1). Ground layers are 50% saturated for the simulation's initialization. (i = ice, t = tundra, fs = various mixed deciduous/evergreen forests, gs = grasslands, ds = desert vegetation, rf = tropical rainforest).

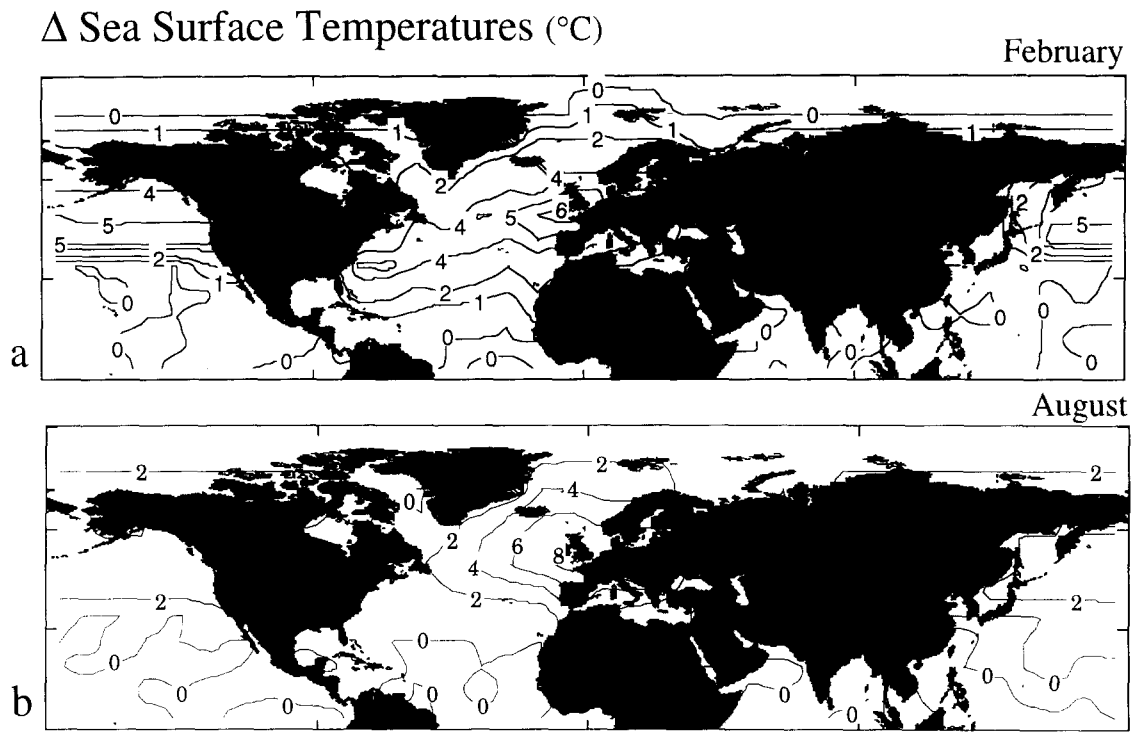
Δ Sea Surface Temperatures (°C)
February
a
August
b

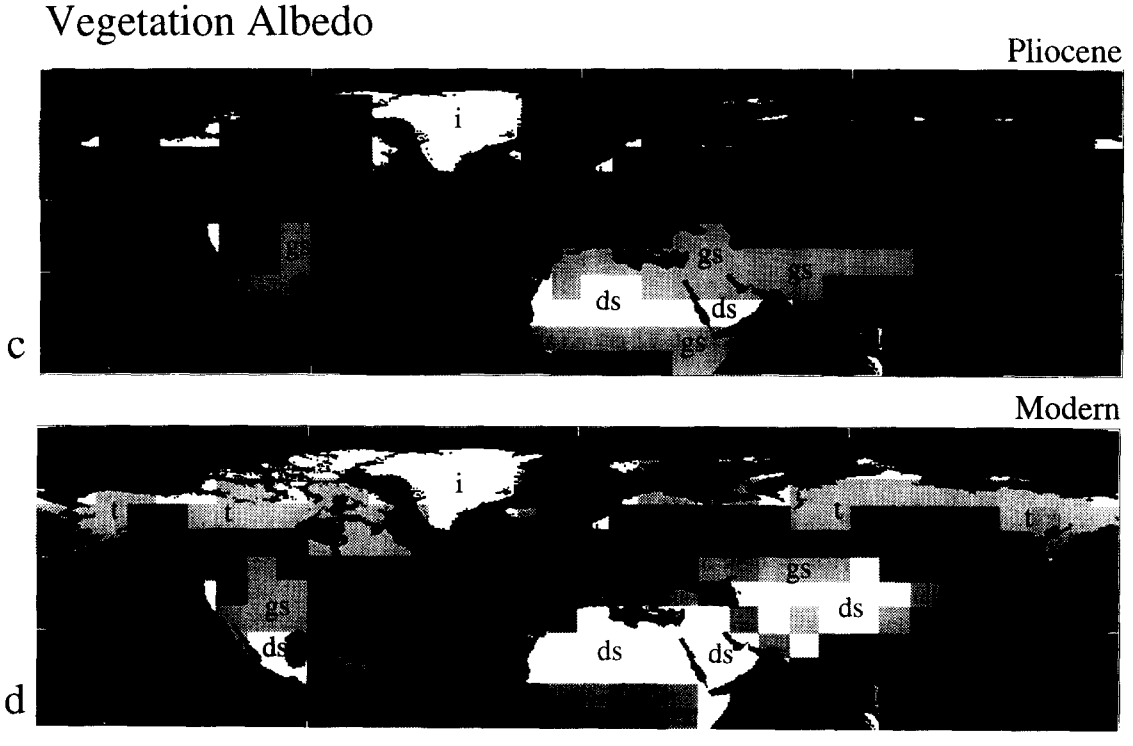
Vegetation Albedo
Pliocene
i
gs
ds
c
Modern
t
d

Table 2
Northern Hemisphere results from three GISS GCM climate simulations

Climate variable	Current	Pliocene	$2 \times CO_2$	% Change		
				Pliocene/ Current	$2 \times CO_2$/ Current	Pliocene/ $2 \times CO_2$
Hydrological cycle (summer)						
Precipitation (mm/day)	3.32	3.49	3.49	5.1%	5.1%	0.0%
over land only	2.96	3.62	3.45	22.3%	16.6%	4.9%
over oceans only	3.67	3.42	3.59	−6.8%	−2.2%	−4.7%
Evaporation (mm/day)	3.02	3.20	3.35	6.0%	10.9%	−4.5%
over land only	2.80	3.32	3.26	18.6%	16.4%	1.8%
over oceans only	3.33	3.14	3.52	−5.7%	5.7%	−10.8%
Snow coverage (%)	2.00	0.50	0.80	−75.0%	−60.0%	−37.5%
Snow depth (m)	1.20	0.30	0.80	−75.0%	−33.3%	−62.5%
Ocean ice coverage (%)	3.30	0.40	2.00	−87.9%	−39.4%	−80.0%
Soil moisture (mm)	56.90	84.50	69.90	48.5%	22.8%	20.9%
Surface runoff (mm/day)	0.90	1.13	1.10	25.6%	22.2%	2.7%
Atmospheric water vapor (10^{-5} kg H_2O/kg	31.50	31.80	40.00	1.0%	27.0%	−20.5%
Cloud properties						
large − scale supersaturated coverage (%)	41.90	40.90	39.20	−2.4%	−6.4%	4.3%
moist convective coverage (%)	10.40	10.50	9.40	1.0%	−9.6%	11.7%
moist convective depth (mb)	440.40	453.60	444.10	3.0%	0.8%	2.1%
Temperature (annual average)						
Surface air temperature (°C)	14.73	16.09	18.78	9.2%	27.5%	−14.3%
Vertically integrated air temperature (°C)	−20.49	−20.48	−16.59	0.0%	−19.0%	23.4%
Equator to pole surface temperature gradient (°C)	46.70	35.20	42.70	−24.6%	−8.6%	−17.6%
Equator to pole vert. integ. temperature gradient (°C)	21.70	18.90	23.20	−12.9%	6.9%	−18.5%
Net radiation at top of atmosphere (W/m^2)	7.50	9.80	7.90	30.7%	5.3%	24.1%
Cloud cover (%)	47.60	46.80	44.80	−1.7%	−5.9%	4.5%
low level	33.70	32.06	32.09	−4.9%	−4.8%	−0.1%
middle level	18.90	18.22	17.23	−3.6%	−8.8%	5.7%
high level	30.25	29.40	29.41	−2.8%	−2.8%	0.0%
Poleward heat transports by:						
—atmospheric eddies (winter)						
Moist static energy (10^{14} W/Δsigma)	29.70	23.20	31.00	−21.9%	4.4%	−25.2%
Dry static energy [10^{14} W/Δsigma]	16.00	12.70	14.60	−20.6%	−8.8%	−13.0%
standing eddies	3.60	3.70	3.50	2.8%	−2.8%	5.7%
transient eddies	12.40	9.00	11.10	−27.4%	−10.5%	−18.9%
Geopotential energy (10^{14} W/Δsigma)	−0.10	−0.20	−0.20	100.0%	100.0%	0.0%
Sensible heat (10^{14} W/Δsigma)	16.10	12.90	14.80	−19.9%	−8.1%	−12.8%
Latent heat (10^{14} W/Δsigma)	13.79	10.48	16.44	−24.0%	19.2%	−36.3%
Eddy kinetic energy (intensity) (10^4 J m^{-2} $\Delta sigma^{-1}$)	131.80	114.40	122.50	−13.2%	−7.1%	−6.6%
standing eddies	17.40	18.90	17.80	8.6%	2.3%	6.2%
transient eddies	114.40	95.50	104.70	−16.5%	−8.5%	−8.8%
—Atmospheric General Circulation (winter)						
Moist static energy (10^{14} W/Δsigma)	411.30	321.80	441.00	−21.8%	7.2%	−27.0%
Dry static energy (10^{14} W/Δsigma)	373.00	299.30	402.40	−19.8%	7.9%	−25.6%
Latent heat (10^{14} W/Δsigma)	38.30	22.50	38.60	−41.3%	0.8%	−41.7%
Kinetic energy (includes eddies) (10^4 J m^{-2} $\Delta sigma^{-1}$)	86.10	71.50	101.40	−17.0%	17.8%	−29.5%
—Oceans (annual average)						
Meridional heat flux, all basins combined (10^{15} W/m^2)	15.00	19.75	15.00 †	31.7%	0.0%	31.7%

Moist static energy = dry static energy + latent heat flux; dry static energy = sensible heat flux + geopotential energy flux
† modern ocean heat transport values were specified in the GISS doubled − CO_2 simulations.

ppm). Nevertheless, the climate forcing potential of increased Pliocene CO_2 should be explored separately, using simulations in which trace gas effects can be studied in a context with full SST and sea ice feedbacks.

3. Middle Pliocene climate: results of GCM experiments

3.1. Temperature

The inclusion of PRISM's Pliocene boundary conditions results in a 1.4°C warming of atmospheric surface air temperatures, averaged over the Northern Hemisphere (Table 2). The warming is amplified at higher latitudes, consistent with the prescribed distribution of SSTs, however, the regional distribution of increased temperatures is not confined to ocean areas (Fig. 3). Zonally averaged, high latitude temperatures increase by more than 10°C in winter, and by 4°C in summer. The largest increases occur between 60°N and 80°N, although, warming of up to 2°C extends into the mid-latitudes and even into the subtropics over Africa. The rise in mid-latitude continental interior temperatures is most pronounced during winter, with increases of between 5°C and 10°C over North America and Asia. Summer temperatures are also warmer, by as much as 4°C, over Canada, central Asia, and western Europe.

Subtropical temperature changes are varied. Minor warming occurs over most of North Africa, Arabia, and northern Mexico during winter and over the western boundary current regions of the oceans throughout the entire year. In contrast to these warmings, air temperatures cool in most subtropical ocean regions. Large temperature decreases also occur regionally, during the summer months, over East Africa and Saudi Arabia, where seasonally average tempera-

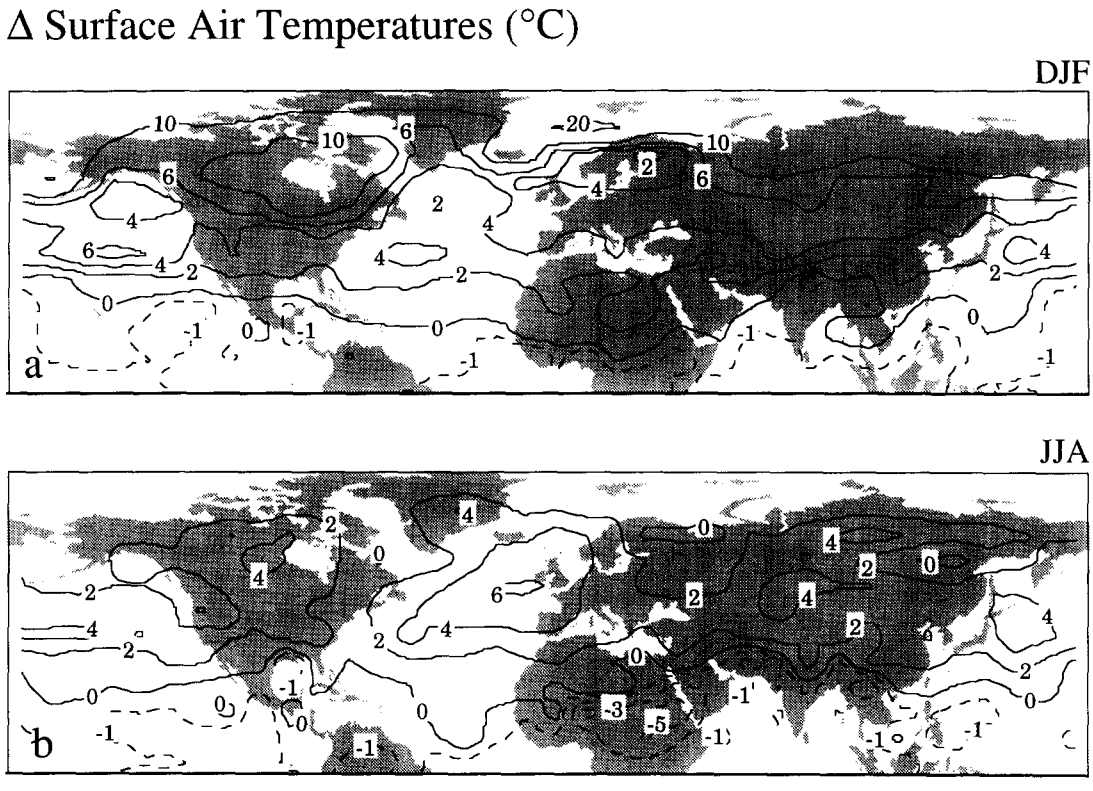

Fig. 3. Surface air temperature change for winter and summer. Unless otherwise noted, results are presented as differences (Δ) between the Pliocene simulation and a GISS GCM current climate control simulation (Hansen et al., 1983). Climate fields are averaged over a given time interval: (a) winter = December, January, February (DJF); (b) summer = June, July, August (JJA); or annual.

tures decline by as much as 6°C. This is a dramatic cooling considering that the specified vegetation changes in that region allow for greater absorption of radiation at the surface (Fig. 2c,d). Tropical temperatures also decrease by approximately 1°C during both summer and winter months despite specified SST values that were virtually unchanged from their modern climatological counterparts.

Vertically integrated temperatures are only slightly altered from those in the current climate experiment (Table 2). The warming effect decreases with height, thus, when vertically integrated, high latitude temperature amplification is less pronounced; the equator to pole air temperature gradient, which decreases by 11.5°C at the surface, changes by only 2.8° when integrated over the entire air column. Above 100 mb the temperature gradient change is actually reversed compared to the change at the surface; warming occurs in the tropical stratosphere and tapers off towards the poles.

3.2. Temperature forcing and feedbacks

The warmer SSTs and reduced sea ice in the high latitude oceans, particularly in the North Atlantic, provide the initial forcing behind the temperature increase in these experiments. Given no other radiative forcing mechanism, the implication is that the observed SST distribution is the result of an increase in the meridional ocean heat transport. The specified Pliocene vegetation patterns (Fig. 2c and Dowsett et al., 1994) decrease surface albedo over the continents and do, also, promote warmer temperatures by increasing the absorption of incoming solar radiation in some regions. During winter, however, the large high to mid-latitude warming in the continental inte-

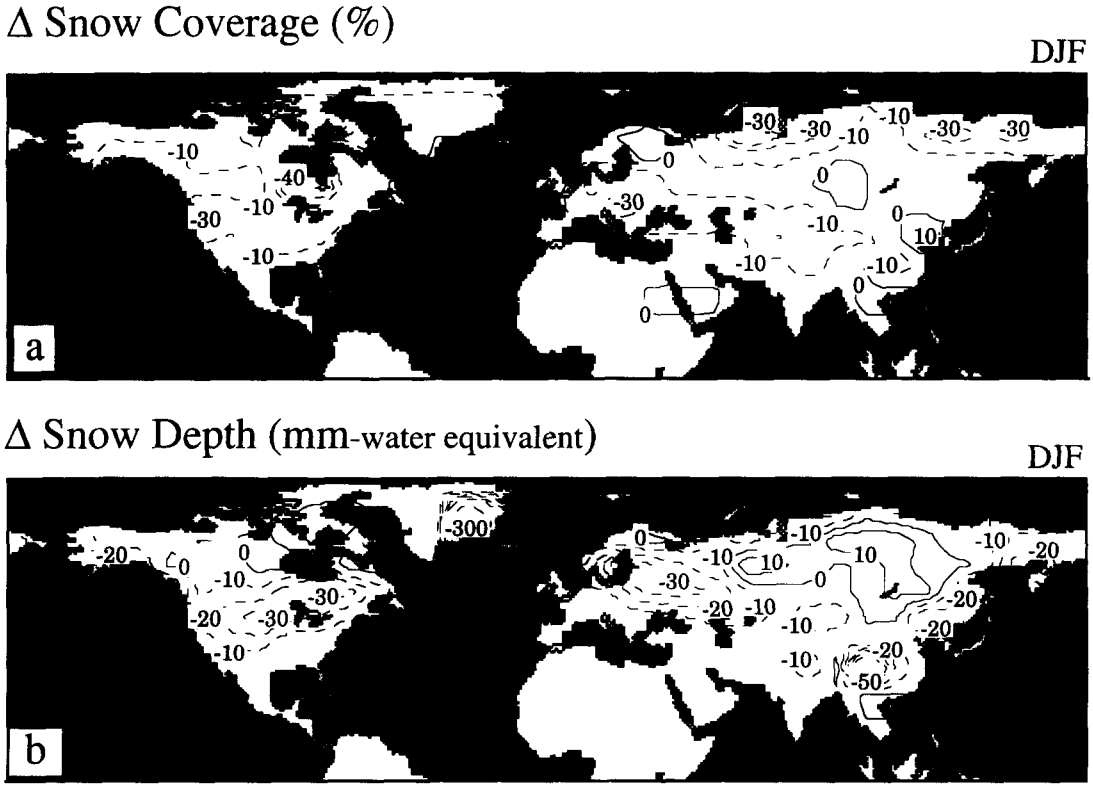

Fig. 4. (a) Snow cover and (b) snow depth change in winter (DJF). Decreased snow cover was a positive feedback in the warmer Pliocene climate simulation. The warmer temperatures reduced snow coverage and shortened the season during which precipitation falls as snow. The reduction in ground albedo allows more solar energy to be absorbed at the surface.

riors is generated primarily by reduced snow coverage and the shortened season of snow accumulation. Decreases in snow cover and snow depth (Fig. 4) alter ground albedos over North America, Europe, and Asia (especially over the Tibetan Plateau) establishing a strong positive feedback in those regions. Albedo changes due to snow reduction are as much as 50% at some latitudes in winter, compared with maximum changes of about 10% due to the altered vegetation patterns. The snow decrease occurs despite an increase in wintertime continental precipitation; most of the precipitation in the warmer Pliocene run falls in the form of rain, not snow. If not for the vegetation changes and the snow–albedo feedback, the generally weaker circulation systems (see below) might actually have lead to cooler and drier continental interiors. Heat and moisture advection have been found to decrease in climates warmed solely by the redistribution of ocean heat (Schneider et al., 1985; Crowley, 1991).

Additional feedback factors, which also play a role in the changes simulated in the Pliocene experiment include adjustments in cloud cover and atmospheric water vapor (Fig. 5 and Table 2). Highly reflective, low level clouds (defined as clouds residing below 720 mb in the GISS GCM) decrease by almost 5% annually, providing a positive feedback that amplifies the warmer climate. Most of that decrease, however, occurs in the extra-tropics while tropical latitudes actually experience increase coverage by low clouds; large increases in cloud cover over Africa are, in fact, responsible for much of the surface temperature decrease in that region. Northern Hemisphere high level clouds (clouds forming above 390 mb) also decrease by a few percent. The change in high level clouds thus serves as a negative feedback to atmospheric warming, since clouds at this height tend to warm the climate (Ramanathan et al., 1989). Despite their potential importance as feedback mechanisms, the cloud cover changes in this simulation should be viewed with caution since the GCM's cloud parameterizations are crude. Compared with available data (which is minimal), the GISS GCM tends to overestimate cloud cover at high latitudes, thus the model's sensitivity at these latitudes may be overestimated. Moreover, variable cloud optical

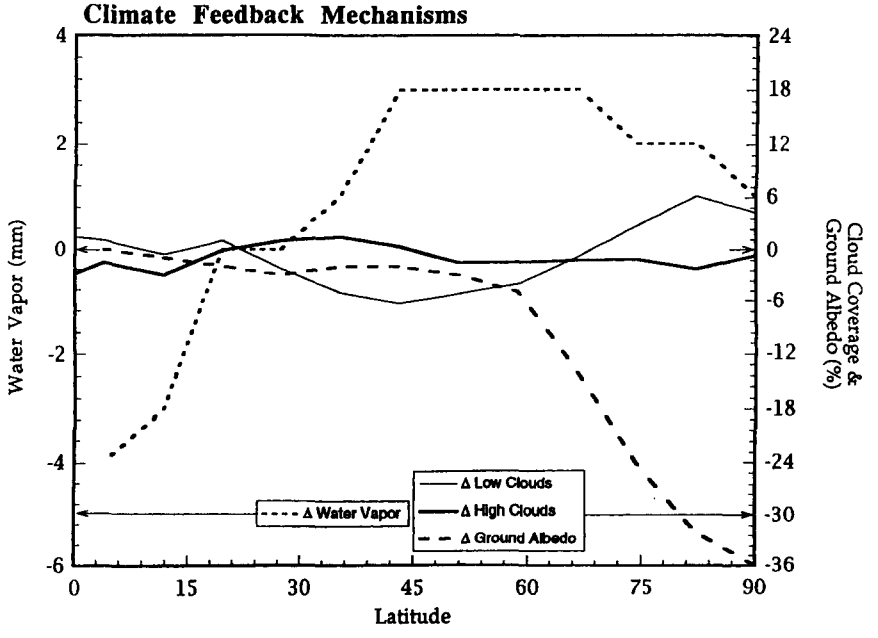

Fig. 5. Pliocene climate feedback mechanisms: change from current climate control run. The primary climate feedbacks that affect warmer climates include cloud distribution, ground albedo (from snow, ice, and vegetation distribution), and atmospheric water vapor. During the Pliocene simulation cloud cover showed little change, water vapor increased north of 18°C but was reduced nearer the equator, and ground albedo was reduced at high latitudes, primarily due to the loss of ice and snow.

properties, which may affect the size and even the sign of the cloud feedback effect, are not predicted by this version of the GCM. Moreover, GCM doubled-CO_2 simulations, which incorporate cloud optical thickness parameterizations, seem to be at odds with recent observations comparing cloud optical thickness change to temperature change (Tselioudis et al., 1992; Tselioudis et al., 1993).

Atmospheric water vapor increase, which constitutes the single most significant positive feedback to warming in doubled-CO_2 climate simulations (Hansen et al., 1984; Rind, 1988), was not as important a factor in our Pliocene simulation; contrast the 1% increase in the Pliocene experiment with the 26% increase in the GISS doubled-CO_2 simulation. The smaller increase in this simulation is the result of the relatively cooler tropical SSTs. The increased SSTs and reduced sea ice at high latitudes do allow for higher evaporation rates, however, Clausius-Clapeyron behavior, which states that cooler air will hold less water vapor per unit temperature increase than warmer air (Wallace and Hobbs, 1977), limits the atmospheric water holding capacity at high latitudes. Since warming in the Pliocene experiment is largely an extratropical phenomenon, large amounts of water vapor are inhibited from entering the atmosphere thus minimizing the water vapor feedback.

3.3. Precipitation and evaporation rates

Northern Hemisphere precipitation rates increase by 5.1% in the Pliocene simulation, a hydrological intensification identical to that found in the GISS doubled-CO_2 experiment (Table 2 and Fig. 6). Precipitation over the ocean decreases slightly (-0.25 mm/day), while the rate over continents rises ($+0.66$ mm/day). The reduced meridional temperature gradient, which decreases storm activity, leads

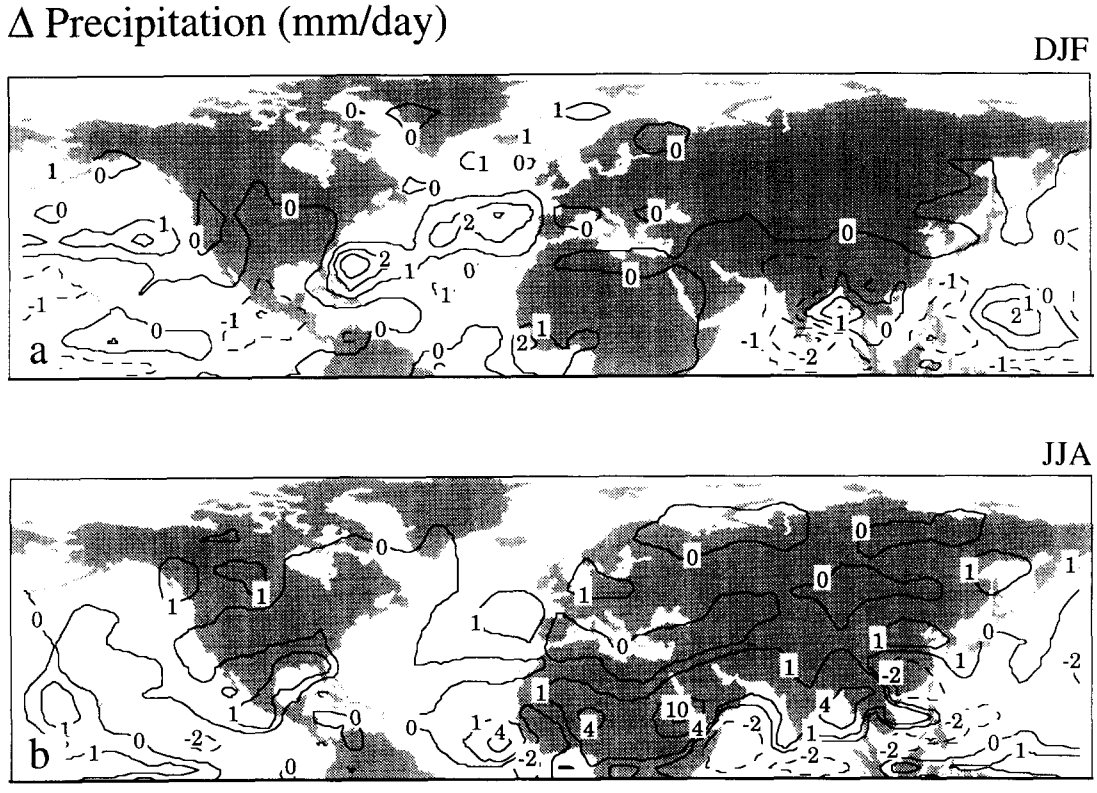

Fig. 6. Precipitation change for winter (DJF) and summer (JJA). Over the oceans, the rainfall anomalies are positive where SSTs were warmer. Large increases in rainfall over subtropical regions resulted primarily from a weakening of the subsidence associated with the Hadley circulation. Warming increased convection over the continents, especially during summer, thus amplifying precipitation increases over land.

to a general reduction of precipitation from large-scale supersaturated clouds, however, a modest increase in moist convective clouds (those which produce most of the rainfall in the model) overcomes the loss due to reduced extra-tropical storms. During winter, precipitation rates over the continents show little change. while, over oceans, major precipitation changes are positively correlated with SST anomalies (Fig. 6). Rainfall increases over the warm ocean regions, particularly in the region surrounding the Gulf Stream, and decreases in the tropics, where no SST warming was specified. During summer the pattern is more complex. Simulated rainfall rates increase substantially throughout the subtropics including extreme intensification over Africa and the Middle East and large increases over the eastern Atlantic and in the Bay of Bengal. In addition, smaller increases occur over central America and northern Canada.

Evaporation rates decrease, on average, over the oceans (Table 2) because the large aerial extent of the subtropics and tropics causes the small decreases in those regions to dominant large evaporation rate increases at high latitudes. The evaporation pattern is responsible for the reduced strength of the water vapor feedback (see above) and it is in stark contrast to the pattern generated in simulations where global warming results from an increase in CO_2 levels. In those scenarios evaporation rates rise throughout the warmer, low latitude ocean areas. The fact, that less atmospheric moisture originates from low latitudes, is evidence that the intensification of continental precipitation must result from the advection of moisture from high latitude waters and, to a large extent,

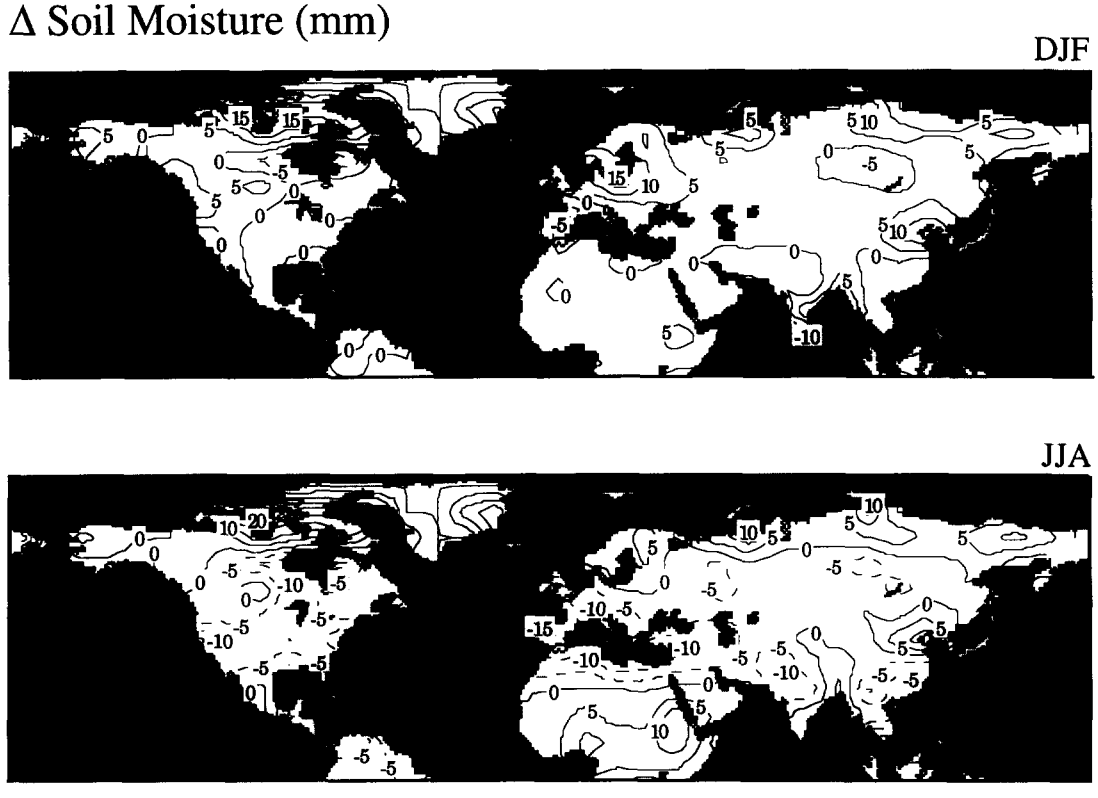

Fig. 7. Soil moisture change for (a) winter (DJF) and (b) summer (JJA). Soil moisture changes are generally positive in winter—a result partially related to the altered Pliocene vegetation boundary conditions, which allowed higher water field capacities in many regions. In contrast, summer soil moisture values in several regions show a decrease compared to the modern climate, a feature related to an increase in evapotranspiration associated with the warmer continental climates. In several locations the model's "summer drought" response is inconsistent with paleobotanical data (see Fig. 14, and Dowsett et al., 1994).

from a recycling of ground moisture. The decreased time over which ground moisture remains frozen and the reduced area of permafrost allows greater amounts of moisture to cycle through the ground layers during a seasonal cycle. Furthermore, with the exception of southeast Asia, each of the regions that experienced large precipitation increases is associated with altered vegetation boundary conditions. Most of the Pliocene vegetation changes yield increased water holding capacities and transpiration efficiency, which reinforces the potential for regional recycling of water (Table 1 and Fig. 2c). The specified vegetation types are consistent with the precipitation rates in those regions, but it is clear that the regional hydrology is heavily dependent upon the vegetation and soil characteristics.

3.4. Soil moisture

Soil moisture responds to the atmospheric demand for water, as well as to its supply, therefore, as a diagnostic variable, it reveals additional aspects of the climate that were not apparent from the precipitation field alone. The simulated soil moisture (defined as the total water in the GCM's two ground layers) is affected by the distribution of vegetation boundary conditions in the GCM because surface albedo, water field capacities and atmospheric exchange rates of the model's ground layers are determined by the specified vegetation (Table 1). Altering the vegetation distribution influences the simulated climate and the climate subsequently influences soil moisture levels.

Soil moisture levels increase throughout the Arctic coastal zone, during both seasons, benefiting from the enhanced hydrological cycle that accompanies the open, warmer high latitude waters (Fig. 7). Similarly, greater advection of moisture from the warmer North Atlantic leads to soil moisture increases in Scandinavian and Northern European during winter. Although generally wetter conditions exist during winter, decreases in soil moisture prevail across the mid latitudes during summer. Subtropical soil moisture change is dominated by the extreme summertime increases in eastern and Sahelian Africa. Notably, however, significant decreases occur in Amazonia and southeast Asia.

The Pliocene soil moisture changes, predictably, are related to the precipitation distribution, but close correspondence is not necessarily universal where other factors come into play. Reduced winter snowfall lessens the springtime meltwater runoff and negatively impacts soil moisture recharge in the upper mid-latitude regions. Magnifying this phenomenon further, less snow cover allows the ground to warm up earlier in the year and moisture is thus lost more rapidly to evaporation and runoff. The seasonal profile of high latitude surface runoff shows that maximum runoff into the Arctic Ocean occurs approximately one month earlier in the Pliocene run than in the current climate control run. Even in areas where precipitation increased during the winter, the soil moisture can become deficit during summer if too little of the winter precipitation was stored as accumulated snow. Areas particularly effected include the region surrounding Hudson Bay, the midwestern United States, and central Canada (Fig. 7). In other areas, including the southern U.S., northern Africa and India, rainfall amounts showed little change; however, soil moisture values decreased considerably. These regions were characterized by increases in moist convective activity. In such systems the rainfall is generally intense and short-lived, resulting in a higher percentage of surface runoff and less soil infiltration. Poleward of 60°N extreme soil moisture increase results partly from higher precipitation rates, but it is also a response to boundary condition changes which, in our experiment, involved replacement of Arctic tundra with boreal forest. The fact that the soil moisture values equilibrated at much higher levels is an indication that the simulated Pliocene climate is consistent with paleoclimate data that suggests expansion of the boreal forest to much higher latitudes. Boreal forest soil types have nearly twice the water holding capacity of the tundras and are capable, therefore, of helping to maintain a wetter regional environment through ground hydrology/atmosphere feedbacks.

3.5. Atmospheric dynamics: eddies

Specifying the warmer high latitude SSTs in the Pliocene experiment implicitly provides an increase of poleward oceanic heat flux. Several studies have shown that increased ocean heat flux is generally accompanied by a compensating decrease in the

atmospheric heat transport (Barron, 1987; Covey and Barron, 1988; Sloan and Barron, 1990; Rind and Chandler, 1991; Chandler et al., 1992). This response, which results because of the reduced latitudinal temperature gradient, is ultimately manifested as a weakening of both the extratropical eddy energy (a measure of storm activity) and the atmospheric general circulation (Table 2). Eddy kinetic energy, in the Pliocene experiment, decreases by over 13% with the peak decrease of 17% occurring at approximately 30°N latitude. Transient eddy energy is reduced nearly twice as much as the energy in standing eddies and this loss of baroclinicity makes it apparent that the altered temperature gradient is the ultimate cause of change. Summertime eddy kinetic energy decreases even more than in winter (−19%); the decline is entirely in the transient eddy component (−25%), while standing eddies actually increase slightly (+8%).

In addition to their intensity, an important activity associated with eddies is the transport of large amounts of energy polewards. Considering the large decreases of eddy kinetic energy it is not surprising that transport of dry static energy by eddies decreases also (Table 2). The reduction is nearly 20% in winter, all in the form of sensible heat loss. It is somewhat surprising that poleward latent heat transports in eddies are also reduced dramatically (24% winter) because atmospheric water vapor actually increases in the Pliocene simulation. However, the additional water vapor is added, primarily, at high latitudes where it is not readily transported by the lower latitude eddies. With warmer SSTs at high latitudes, and little or no warming at low latitudes, the Pliocene atmospheric water vapor is actually decreased at all zones equatorward of 40° (Fig. 5). This characteristic is in sharp contrast to the situation produced in doubled-CO_2 global warming experiments (Rind, 1987b). In GISS doubled-CO_2 simulations, despite reduced summertime eddy intensity, there is no loss of latent heat transport because low latitude SSTs warm, generating much higher tropical water vapor levels. During winter, eddy latent heat transports actually increase by over 50% in the dou-

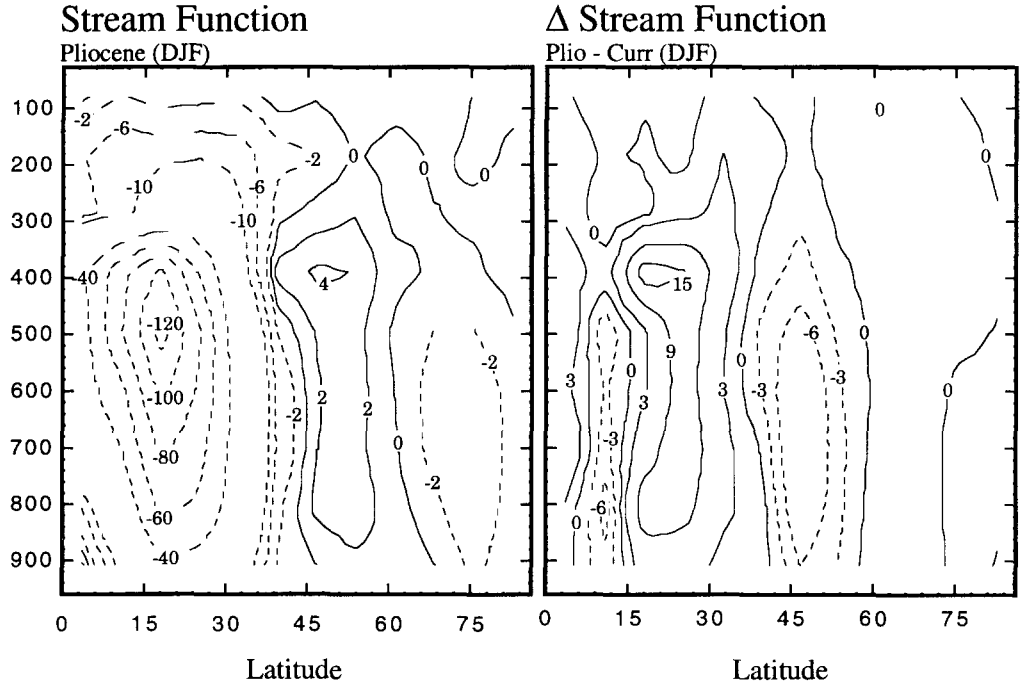

Fig. 8. (left) Stream function (negative values represent clockwise flow) and (right) the change in stream function [10^9 kg/sec] for Northern Hemisphere winter. The stream function is a representation of the atmospheric mass flux and is commonly used to visualize primary features of the general circulation. Changes in the stream function for the Pliocene climate reveal an overall weakening of both the thermally direct, low latitude Hadley cell and the mid-latitude Ferrel cell.

bled-CO_2 climate. The difference between the two warm climate scenarios is more than quantitative; in the doubled-CO_2 simulation, latent and sensible heat transports are a positive feedback, augmenting high latitude temperature amplification, while in the Pliocene run, altered energy transports act as a negative feedback to high latitude warming.

3.6. Atmospheric dynamics: general circulation

In addition to affecting eddy transports, the smaller temperature gradient, particularly between the tropics and subtropics, has the effect of weakening the large-scale atmospheric general circulation (Fig. 8). The Hadley Cell's intensity is reduced by 11%, diminishing the rising motion in the tropics and subsidence over the subtropics. Subtropical subsidence is lessened in the Pliocene run; however, this does not substantially increase subtropical precipitation, presumably because wave energy, which triggers instability and rainfall events, is reduced. In contrast, during the summer, the reduced subtropical subsidence contributes to an enormous increase in rainfall over northern Africa, Arabia, India and southeastern Asia. The thermally-indirect Ferrel Cell is also reduced compared with the control run, although the model's Ferrel Cell is too weak even in the current climate simulation.

At extratropical latitudes, the effects of other forces, such as warmer SSTs, reduced sea ice, and less snow, are felt directly. The Icelandic low deepens (Fig. 9), as the warm, ice-free waters of the North Atlantic destabilize the atmosphere in that vicinity. Similarly, the Aleutian low strengthens, albeit to a lesser extent. The Siberian High weakens in response to the regional warming caused by the

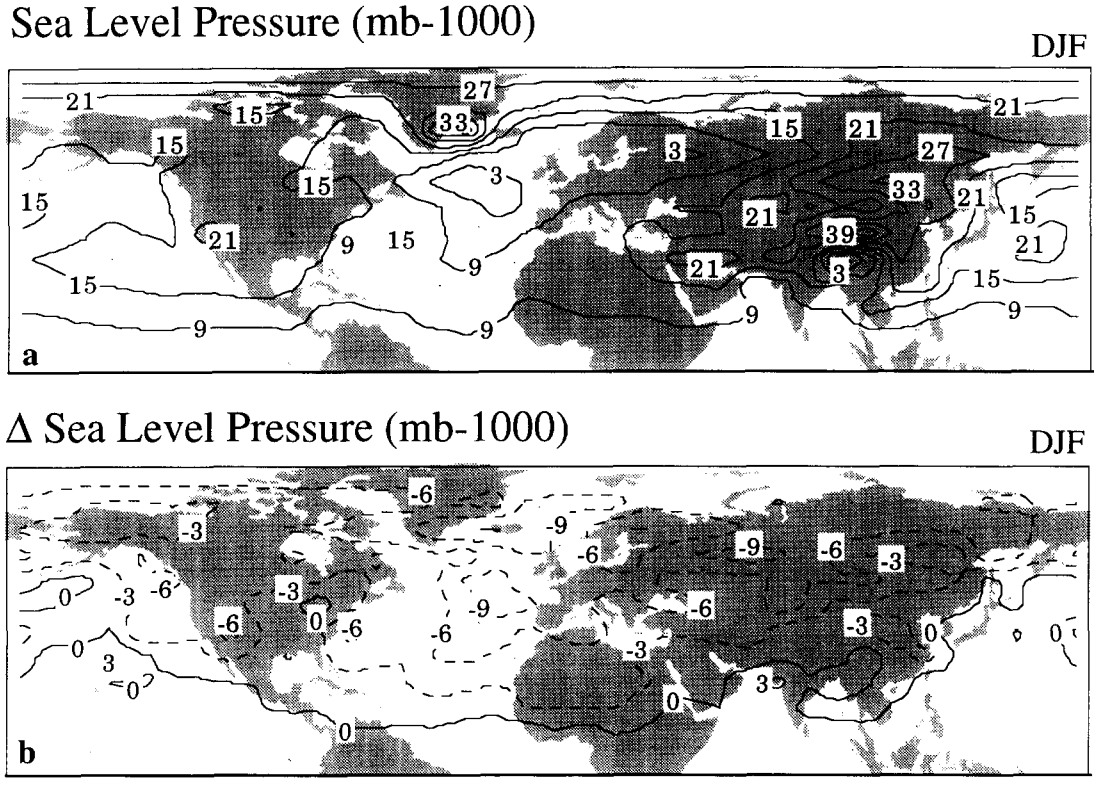

Fig. 9. (a) Winter season sea level pressure field for the Pliocene simulation and b) Pliocene sea level pressure change from the GISS current climate control run. Pressures are lower over much of the Northern Hemisphere; warmer SSTs destabilize the lower atmosphere, deepening the Icelandic and Aleutian lows. High pressure cells over North America and Siberia are weakened by the continental warming associated with reduced winter snow cover (see Fig. 4).

reduced snow cover and dampened snow/albedo feedback. The feedback is strong enough that it actually increases the land/ocean contrasts despite the warmer ocean temperatures. This effect is most evident between North America and the North Atlantic.

Zonal wind speeds in the Pliocene decrease slightly at all of the upper levels (Fig. 10). The mid-latitude jet stream weakens by approximately 4 m/s at its peak, but the maximum does not shift appreciably from its current simulated position at 30°N. Farther north, high altitude winds diminish by about the same amount as the mid-latitude jet stream. Surface winds in both summer and winter show patterns that are broadly similar to the present in terms of direction (Fig. 11), although the magnitudes generally show weakening over the continents and in the tropics. Variable increases are seen over regions of North America, Siberia, and the Tibetan plateau where reduced snow cover (Fig. 4) altered the surface heating (Fig. 3). The largest changes occur over the oceans where winds are actually strengthened during both seasons in regions affected by the Icelandic and Aleutian lows. To a lesser degree, winds were strengthened in response to the enhancement of high pressure zones over subtropical ocean regions. Smaller changes, with less consistent patterns, are typical over North America, Eurasia and Siberia in winter, reflecting the weakening of extratropical high pressure cells.

4. Discussion: increased ocean heat transport and warmer climates

Specifying SSTs as a boundary condition in GCM climate experiments is useful in that it forces the atmosphere to react to the appropriate ocean surface fluxes (assuming the SSTs are known) and it is computationally more efficient than using mixed-layer or fully coupled ocean models. Yet the practice removes the potential feedback contribution of the oceans, which can otherwise adjust to the climate changes calculated by the GCM.

In their review of the climatic role played by ocean heat transports, Covey and Barron (1988)

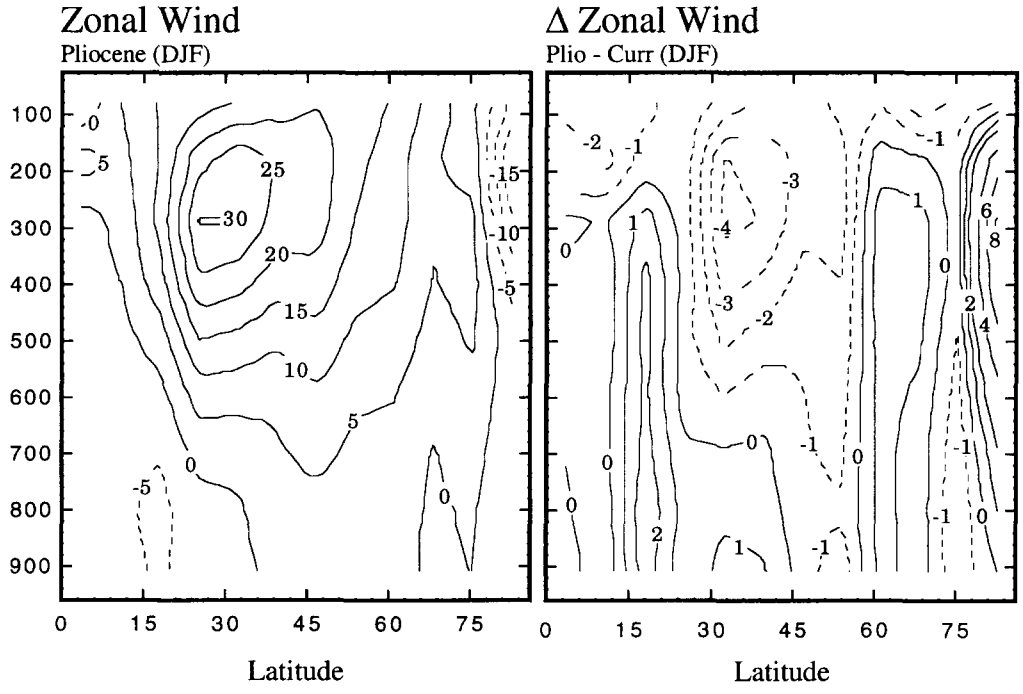

Fig. 10. (a) Zonal wind in m/s (positive values represent westerly winds) and (b) change in zonal wind (m/s) for Northern Hemisphere winter. The dampened equator to pole temperature gradient reduces the strength of the jet level winds in accordance with the thermal wind equation. Zonal averages reveal no shift in the latitude of peak jet intensity.

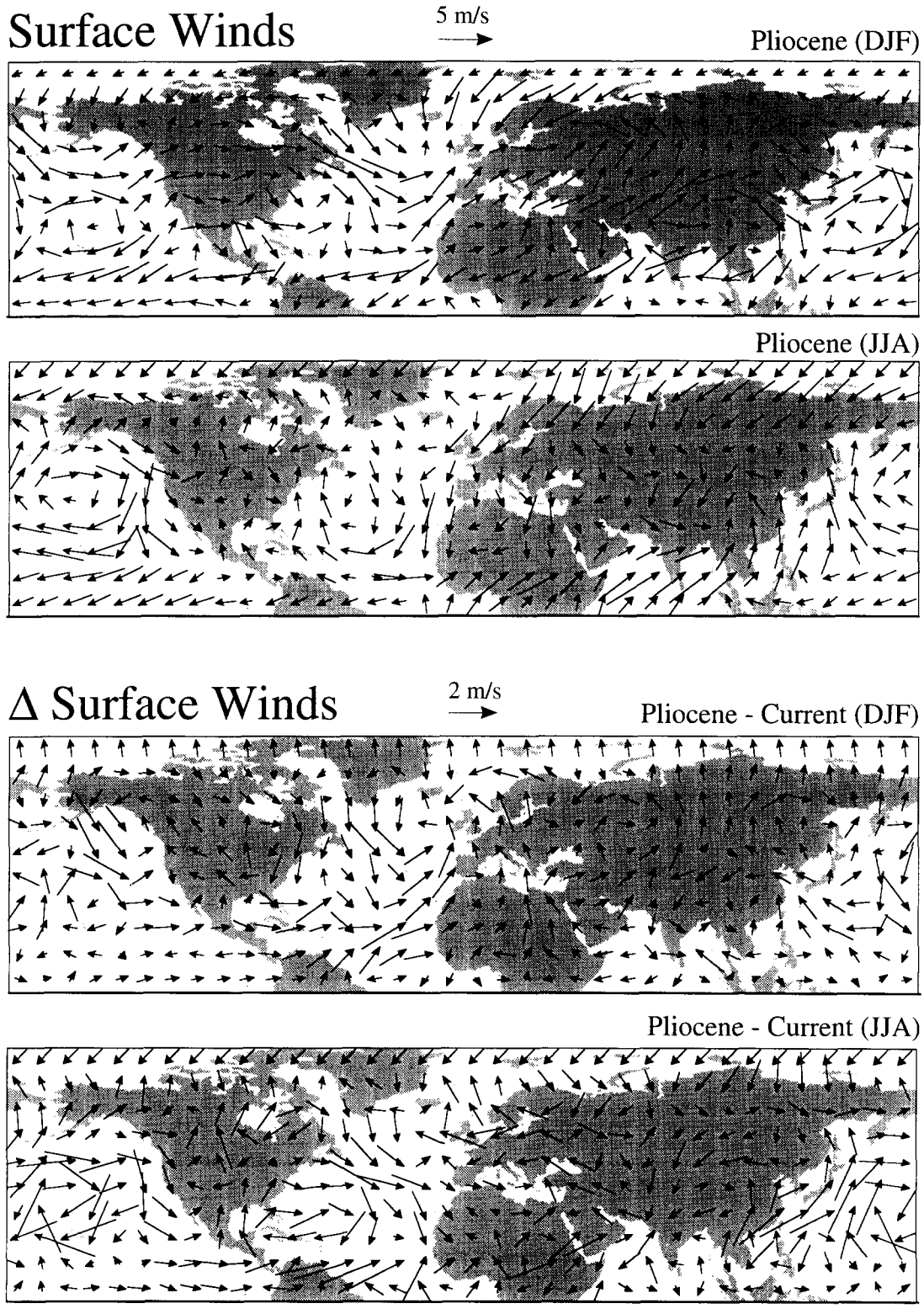

Fig. 11. Surface wind patterns and change of surface winds for winter (DJF) and summer (JJA). Responding to pressure changes (see Fig. 8) the Pliocene surface winds are generally increased about the major stationary cells. One exception may be in the tropical Atlantic where an intensified African monsoon appears to weaken the trade winds.

pointed out that experiments using specified SSTs represent an arbitrary scenario since "the [implied] ocean heat transport does not reflect the model boundary conditions of energy put into the system but rather implies some additional energy source and mechanism of energy redistribution". In effect, if specified SSTs were, instead, coupled to the GCM's atmosphere they would adjust until the radiation emitted by the oceans balanced the atmospheric energy flux. As mentioned above, it has been shown that atmospheric transports tend to compensate for additional energy transport by the oceans, thus, without an additional radiative energy source (increased CO_2 or solar radiation perhaps) warm specified ocean temperatures would, presumably, cool. At the time, Covey and Barron concluded that "the potential role of ocean heat transport to explain past climates is probably overstated". Still, they suggested that a more useful way of studying the problem would be to use explicitly supplied ocean heat transports in a GCM.

When such experiments were conducted (Rind and Chandler, 1991) it was shown that increased ocean heat transports could produce snow/albedo and sea ice/albedo feedbacks that compensated, or even overcompensated, for the energy imbalances created by the warmer SSTs and weakened atmospheric dynamics. The conclusion was that certain warm SST scenarios could be self-sustaining if alternate modes of ocean circulation were proved to be plausible. Moreover, additional radiative forcing, beyond that produced by the ocean heat transport feedbacks, appears to be unnecessary in order to sustain otherwise arbitrary SST specifications. Thus, for many warmer climates, past or future, the primary concern lies with the plausibility of the ocean heat transport scenario, whether implied or explicit. Some warm SST scenarios, such as Barron's Cretaceous experiments, using 10°C polar SSTs, are thought to be implausible, as they require enormous transports across relatively small latitudinal zones (Covey and Barron, 1988). However, Barron (1983) concluded that Cretaceous ocean heat transports, sufficient to melt all polar sea ice, were, theoretically, possible.

Pliocene albedo feedbacks generated an additional 2 Wm^{-2} beyond that needed to sustain the specified SSTs. Given the GISS GCM's sensitivity of approximately 1°C $W^{-1}m^{-2}$ (Hansen et al., 1984), the simulated Pliocene climate would have warmed an additional 2°C if explicit, rather than implied, ocean heat transports had been employed. If the PRISM Pliocene SST distribution is assumed to have been generated entirely by altered ocean circulation, the required increase of poleward ocean heat flux would be approximately 32% in the Northern Hemisphere (Fig. 12). Rind and Chandler (1991) and Covey (1991) have suggested that increases of this magnitude are plausible, but that wind driven circulation, thermohaline circulation, or both would have to be altered to generate the change. Coupled ocean–atmosphere GCMs will, eventually, be employed to analyze such questions; however; current ocean models cannot accurately simulate deepwater production without resorting to restoration functions or flux corrections. In lieu of this option, we can at least identify whether or not the simulated Pliocene atmospheric regime positively or negatively reinforces the primary ocean circulation mechanisms.

Fig. 13 shows the annually averaged difference (Pliocene minus modern) for variables that affect ocean circulation: surface winds, surface temperature, and moisture balance. Surface wind changes (Fig. 13a) are large over the oceans and, therefore, might be expected to alter ocean surface circulation. Wind velocities increased over western boundary currents of the Atlantic and Pacific oceans, which is suggestive of increased heat flux in those major, poleward flowing, water masses. However, smaller counter currents are enhanced on the open ocean

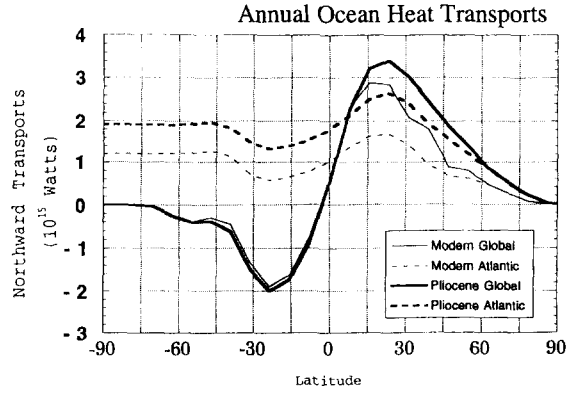

Fig. 12. Pliocene and modern ocean heat transports for all oceans combined (global) and for the Atlantic Ocean alone. Transports were calculated based on the surface energy balances obtained from the GCM using the method of Miller et al. (1983).

sides of both the Gulf Stream and the Kuroshio currents. Tropical easterly winds in the Pacific show a slight tendency to increase the east to west flow in that ocean but, over the Atlantic, the strong reversal of trade winds, caused by the enhanced African monsoon, implies a weakened tropical ocean circulation. At high latitudes, the deepened Icelandic low is the dominant feature and produces stronger winds that could enhance circulation in the North Atlantic and Greenland Sea. To the extent that this would limit the poleward encroachment of the Gulf Stream waters, this may prove to be a negative feedback to high latitude warming.

The SST changes shown in the PRISM data set (see Fig. 2a,b and Dowsett et al., 1994) are dominated by warmer high latitude temperatures, which

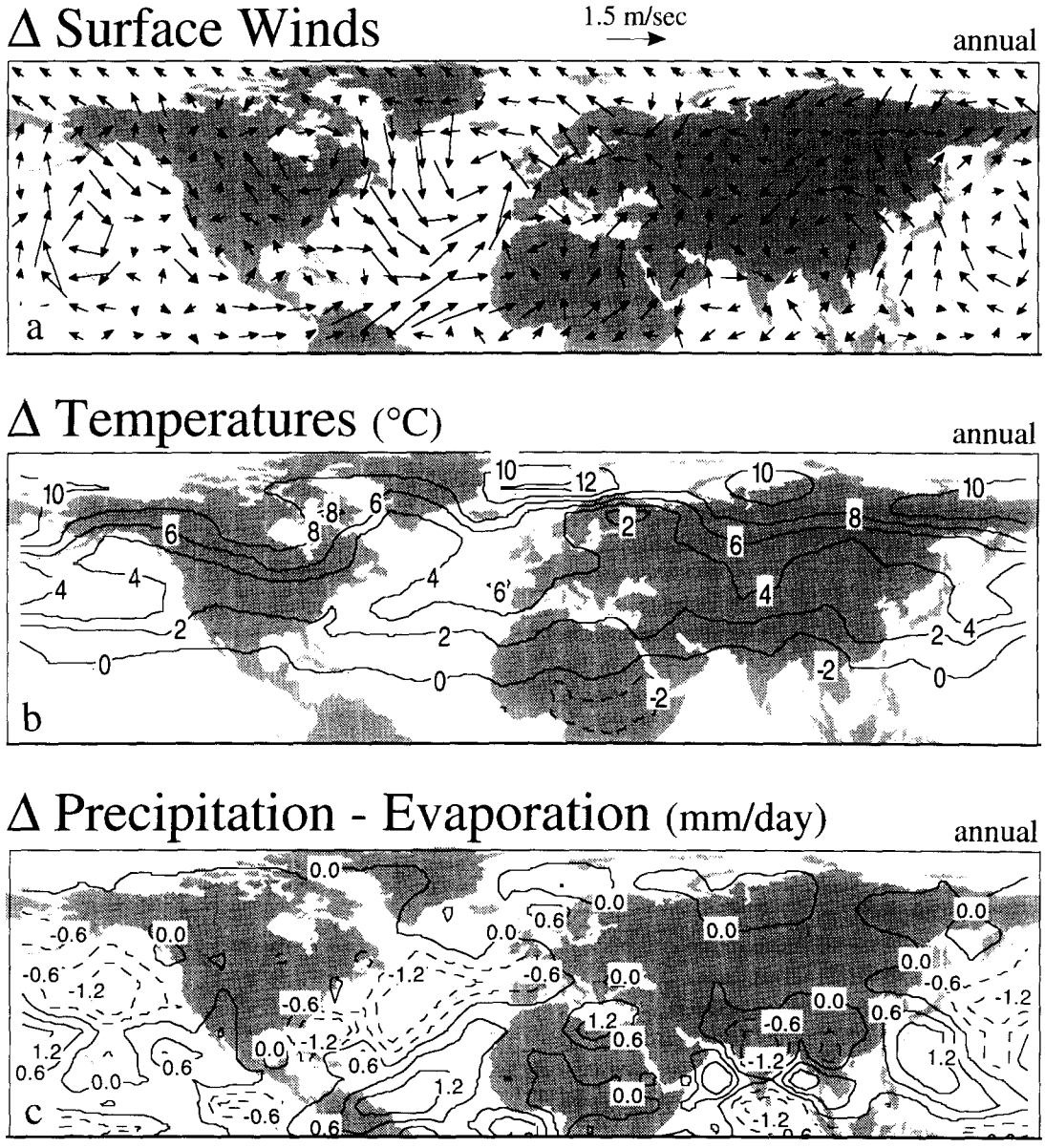

Fig. 13. Annually averaged differences between Pliocene and current climate control runs for values that influence ocean circulation and, therefore, meridional ocean heat transports: (a) surface winds, (b) surface temperature, (c) precipitation minus evaporation.

likely would result in a more stable ocean in the regions of the North Atlantic where deep water formation is most common. The warmer SSTs lead to significantly warmer surface air temperatures (Fig. 13b), particularly at high latitudes; fewer cold days and increased minimum temperatures would decrease average surface water density and reduce the opportunities for deep water production. Furthermore, the reduced area over which sea ice forms might short circuit the salinity increases that can occur when freshwater is removed from the surface ocean during freezing. Looked at in another way, these same processes might shift the locus of deep water production poleward, allowing more heat to be imported into higher latitudes.

Finally, changes in the moisture balance over the oceans (Figure 13c) strongly support an increase of salinity at middle to high latitudes and, potentially, an intensified Pliocene thermohaline circulation. Over the North Atlantic, between 40°N and 70°N, the moisture balance shows a change of 107% towards more evaporative conditions. Covey and Barron (1988) suggested that the thermohaline circulation might provide as much as half of the current poleward ocean heat transports; if so, the altered moisture fluxes, alone, might be enough to increase the poleward ocean heat flux by the required 15–20%. In fact, some experiments with the GISS GCM (Rind and Chandler, 1991) suggested that increasing Atlantic transports by as little as 36% might be enough to melt all Arctic sea ice and could create a warm climate similar to our Pliocene simulation. Further conjecture awaits ocean–atmosphere models that can simulate deep water production without resorting to the types of extreme surface flux corrections currently required by ocean GCMs.

5. Conclusions

Comparisons of the simulated regional climatic features with Pliocene paleoclimate data in Fig. 14 indicate that surface air temperatures produced by the GCM in the Northern Hemisphere closely approximate palynological temperature estimates. The general pattern of surface air warming follows from the SST patterns that were specified using PRISM data (Dowsett et al., 1994); little change in the tropics with amplification at high latitudes. Greatest warming occurs in the northern extremes of North America and Russia, as well as in Northern Europe, where temperatures rise 12°C in some locations.

The altered SST gradient strongly implicates ocean heat transports as a driving force behind the middle Pliocene warmth. Levels of CO_2, large enough to cause such extreme high latitude temperatures, would generate concomitant warming in tropical regions—a warming that is not evidenced by paleorecords. Calculated surface fluxes show that an increased meridional ocean heat flux of not quite 32% could achieve a climate similar to the one portrayed by the PRISM data. Given the warmer high latitude waters and the sluggish state of the atmosphere, which results from the reduced latitudinal temperature gradient, any ocean flux increase would probably have resulted from a strengthening of the thermohaline circulation through salinity increases.

Continental warming is enhanced during the winter by reductions in both snow and sea ice, which generates a positive albedo feedback. In no continental regions are simulated temperatures substantially cooler than the data imply. This is in contrast to many other warm paleoclimate scenarios for which model/data comparisons have been conducted. Data for many past time periods (e.g. Cretaceous, Jurassic, Eocene) portray continental interior temperatures as having been much warmer than any GCMs are able to produce, using reasonable boundary conditions (Barron and Washington, 1985; Chandler et al., 1992; Sloan and Barron, 1990). Interpretations of continental interior warming for the Pliocene does not tend to be as extreme as for some of the earlier warm periods, but the similarity between Pliocene and modern continental boundary conditions suggests that any tuning parameters built into the GCM are also more likely to be valid. Ultimately, we expect a good match between model-derived and data-derived temperature fields, because temperatures are generally a robust diagnostic in the GCM. Furthermore, temperatures are not modified at the local scale as much as other climate variables, thus site-specific data, such as palynological records, are more representative of regional conditions.

Conversely, hydrological characteristics exhibit great regional variability, making it harder to extrap-

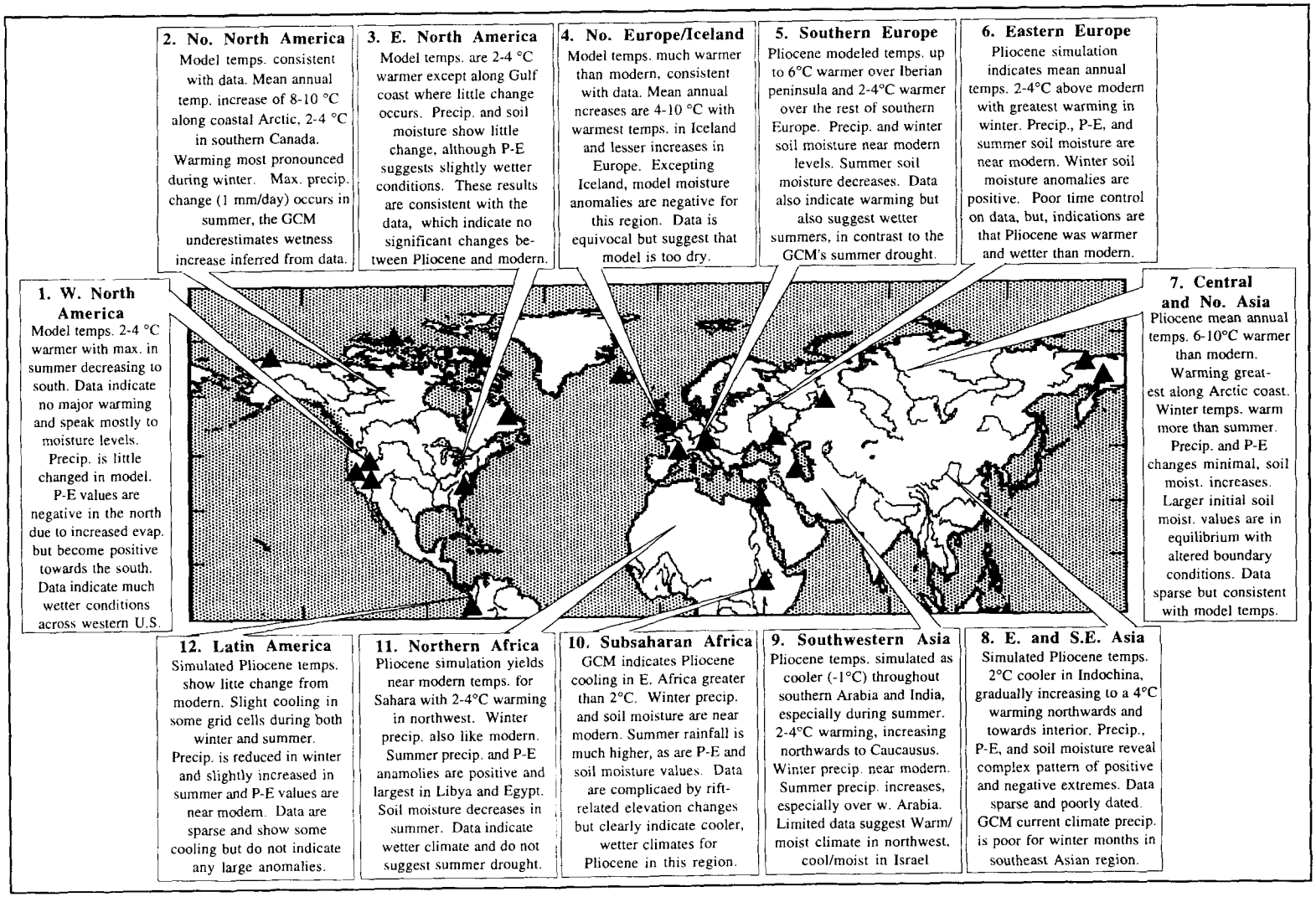
2. No. North America
Model temps. consistent with data. Mean annual temp. increase of 8-10 °C along coastal Arctic, 2-4 °C in southern Canada. Warming most pronounced during winter. Max. precip. change (1 mm/day) occurs in summer, the GCM underestimates wetness increase inferred from data.
3. E. North America
Model temps. are 2-4 °C warmer except along Gulf coast where little change occurs. Precip. and soil moisture show little change, although P-E suggests slightly wetter conditions. These results are consistent with the data, which indicate no significant changes between Pliocene and modern.
4. No. Europe/Iceland
Model temps. much warmer than modern, consistent with data. Mean annual ncreases are 4-10 °C with warmest temps. in Iceland and lesser increases in Europe. Excepting Iceland, model moisture anomalies are negative for this region. Data is equivocal but suggest that model is too dry.
5. Southern Europe
Pliocene modeled temps. up to 6°C warmer over Iberian peninsula and 2-4°C warmer over the rest of southern Europe. Precip. and winter soil moisture near modern levels. Summer soil moisture decreases. Data also indicate warming but also suggest wetter summers, in contrast to the GCM's summer drought.
6. Eastern Europe
Pliocene simulation indicates mean annual temps. 2-4°C above modern with greatest warming in winter. Precip., P-E, and summer soil moisture are near modern. Winter soil moisture anomalies are positive. Poor time control on data, but, indications are that Pliocene was warmer and wetter than modern.
1. W. North America
Model temps. 2-4 °C warmer with max. in summer decreasing to south. Data indicate no major warming and speak mostly to moisture levels. Precip. is little changed in model. P-E values are negative in the north due to increased evap. but become positive towards the south. Data indicate much wetter conditions across western U.S.
7. Central and No. Asia
Pliocene mean annual temps. 6-10°C warmer than modern. Warming greatest along Arctic coast. Winter temps. warm more than summer. Precip. and P-E changes minimal, soil moist. increases. Larger initial soil moist. values are in equilibrium with altered boundary conditions. Data sparse but consistent with model temps.
12. Latin America
Simulated Pliocene temps. show litte change from modern. Slight cooling in some grid cells during both winter and summer. Precip. is reduced in winter and slightly increased in summer and P-E values are near modern. Data are sparse and show some cooling but do not indicate any large anomalies.
11. Northern Africa
Pliocene simulation yields near modern temps. for Sahara with 2-4°C warming in northwest. Winter precip. also like modern. Summer precip. and P-E anamolies are positive and largest in Libya and Egypt. Soil moisture decreases in summer. Data indicate wetter climate and do not suggest summer drought.
10. Subsaharan Africa
GCM indicates Pliocene cooling in E. Africa greater than 2°C. Winter precip. and soil moisture are near modern. Summer rainfall is much higher, as are P-E and soil moisture values. Data are complicaed by rift-related elevation changes but clearly indicate cooler, wetter climates for Pliocene in this region.
9. Southwestern Asia
Pliocene temps. simulated as cooler (-1°C) throughout southern Arabia and India, especially during summer. 2-4°C warming, increasing northwards to Caucausus. Winter precip. near modern. Summer precip. increases, especially over w. Arabia. Limited data suggest Warm/moist climate in northwest, cool/moist in Israel
8. E. and S.E. Asia
Simulated Pliocene temps. 2°C cooler in Indochina, gradually increasing to a 4°C warming northwards and towards interior. Precip., P-E, and soil moisture reveal complex pattern of positive and negative extremes. Data sparse and poorly dated. GCM current climate precip. is poor for winter months in southeast Asian region.

olate from site-data to large areas such as those represented by a GCM grid cell. Globally averaged, evaporation and precipitation decrease over the oceans, although large positive anomalies are dominant at high latitudes where increased evaporation tends to exceed the change in precipitation. The hydrological cycle intensifies over the continents, where annual average evaporation, rainfall, and soil moisture all increase. Summer drought is, however, a regular feature of the Pliocene experiment, a result that is not supported by terrestrial records and which points to deficiencies in hydrological parameterizations and perhaps in assigned boundary conditions. The model's simple parameterizations for clouds, convection, and ground hydrology make simulated precipitation, soil moisture, and runoff less reliable, yet, hydrological results from East Africa, Europe, eastern North America, and Canada, are consistent with paleorecords (Fig. 14). In some regions, where hydrological data and model results are mismatched, such as the western U.S., problems are exacerbated by the high relief topography. A fractional grid GCM, as was used here, resolves topographic features better than a spectral model of similar resolution, but, significantly finer resolutions are required in order to distinguish relief of the type that exists in the Basin and Range. Because the data is sparse, and necessarily local in nature, and because the computational expense of reducing resolution is extreme, experiments like those conducted recently by Hostetler et al. (1994), using nested-grid resolutions, may be the most reasonable near term solution for improving hydrological paleoclimate data-model comparisons.

The GCM simulation identifies specific areas such as north Africa, central and southeast Asia, and Central America for future data collection because further analyses in those regions could help validate simulated climate changes. Our study also emphasizes the requirement for global data sets and quantitative estimates of climate related parameters for model/data studies. The Pliocene model-data comparison project employs an iterative, cooperative approach, and this study represents only the first step. Already, the Northern Hemisphere PRISM data, presented in Dowsett et al. (1994), are being expanded and refined to include estimates for the Southern Hemisphere and more sophisticated versions of the GISS GCM are being prepared for future experiments.

Despite constant need for more computational power, the pace of such projects is limited mostly by the time consuming process of obtaining and analyzing new data. It is hoped that the GCM can help speed this process by identifying critical sites for exploration or reanalysis. The Pliocene remains an essential time period to understand, because it is the most recent period in geologic history having temperatures as warm as those anticipated for the coming century. In many respects, from continental distribution to vegetation types, it is more similar to our future than any other warm period of the past. More data and simulations are needed, and we must explore controversial issues within both the data and modeling segments of the project; however, it is likely that we will add to our ability to predict future climate change as we improve our capability to simulate the Pliocene.

Fig. 14. Qualitative comparisons between Pliocene simulation results and terrestrial records for several large geographic regions of the Northern Hemisphere. The text of this paper contains a more detailed discussion of model results while further discussion of the data may be found in the companion paper by Dowsett et al. (1994) as well as in the references listed below. References are numbered to correspond with a specific region in the above figure and full citations appear in the reference list of Dowsett et al. (1994): 1. Adam et al., 1989, 1990; Smith et al., 1993; Smith, 1984; Thompson, 1991; Thompson, 1992; Winograd et al., 1985. 2. De Vernal and Mudie 1989a, b; Matthews 1987, 1990; Matthews and Ovenden, 1990; Nelson and Carter, 1985. 3. Groot 1991; Litwin and Andrle, 1992; Willard et al.,1993; Willard (in review). 4. Iceland—Akhmetiev et al., 1978; Akhmetiev, 1991; Schwarzbach and Pflug, 1957; Willard, 1992; Willard (in review). Northern Europe—Hunt, 1989; Mohr, 1986; Rousseau et al., 1992; Suc and Zagwijn, 1983; Zagwijn, 1992; Zalasiewicz et al., 1988. 5. Bertolani Marchetti, 1975; Bertolani Marchetti et al., 1979; Cravatte and Suc, 1981; Gregor 1990; Suc and Zagwijn, 1983; Suc, 1984. 6. Grichuk, 1991; Planderová, 1974; Stuchlik and Shatilova, 1987; Traverse, 1982. 7. Fradkina, 1991; Giterman et al., 1982; Tanai and Huzioka, 1967; Volkova, 1991. 8. no evidence. 9. Horowitz, 1989; Horowitz and Horowitz, 1985; Mamedov, 1991; Quade et al., 1989; Shatilova, 1980, 1986; Shatilova et al., 1991. 10. Bonnefille et al., 1987; Cerling, 1992; Cerling et al., 1988; Williamson, 1985. 11. Maley, 1980; Sarnthein et al., 1982; Suc and Zagwijn, 1983. 12. Graham, 1989; Hooghiemstra, 1989; Hooghiemstra and Sarmiento, 1991.

References

Amano, K. and Taira, A., 1993. Reply to Comment on: Two-phase uplift of Higher Himalayas since 17 Ma. Geology, 21: 379.

Barron, E.J., 1983, The oceans and atmosphere during warm geologic periods. Proc. Joint Oceanographic Assembly 1982, General Symposia. Can. Natl. Comm. Ocean Res., Ottawa, Ont., 189 pp.

Barron, E.J., 1987. Eocene equator-to-pole surface ocean temperatures: A significant climate problem? Paleoceanography, 2: 729–739.

Barron, E.J., 1989. Studies of Cretaceous Climate. In: A. Berger, R.E. Dickinson and J.W. Kidson (Editors), Understanding Climate Change. Am. Geophys. Union, Washington, DC, pp. 149–158.

Barron, E.J. and Peterson, W.H., 1990. Mid-Cretaceous ocean circulation: Results from model sensitivity studies. Paleoceanography, 5: 319–338.

Barron, E.J. and Washington, W.M., 1984. The role of geographic variables in explaining paleoclimates: results from Cretaceous climate model sensitivity experiments. J. Geophys. Res., 89: 1267–1279.

Barron, E.J. and Washington, W.M., 1985. Warm Cretaceous climates : High atmospheric CO_2 as a plausible mechanism. In: E.T. Sundquist and W.S. Broecker (Editor), The Carbon Cycle and Atmospheric CO_2: Natural Variations Archean to Present (Geophys. Monogr., 32). Am. Geophys. Union, Washington, DC, pp. 546–553.

Chandler, M.A., Rind, D. and Ruedy, R., 1992. Pangaean climate during the Early Jurassic: GCM simulations and the sedimentary record of paleoclimate. Geol. Soc. Am. Bull., 104: 543–559.

Cochran, J.R., 1993. Comment on: Two-phase uplift of Higher Himalayas since 17 Ma. Geology, 21: 378–379.

Covey, C. and Barron, E.J., 1988. The role of ocean heat transport in climatic change. Earth-Sci. Rev., 24: 429–445.

Covey, C., 1991. Climate change: Credit the oceans? Nature, 352: 196–197.

Crowley, T.J., 1991. Modeling Pliocene warmth. Quat. Sci. Rev., 10: 275–282.

Dowsett, H.J. and Cronin, T.M., 1990. High eustatic sea level during the middle Pliocene: evidence from southeastern U.S. Atlantic coastal plain. Geology, 18: 435–438.

Dowsett, H.J., Cronin, T.M., Poore, R.Z., Thompson, R.S., Whatley, R.C. and Wood, A.M., 1992. Micropaleontological evidence for increased meridional heat transport in the North Atlantic Ocean during the Pliocene. Science, 258: 1133–1135.

Dowsett, H.J., Thompson, R.S., Barron, J.A., Cronin, T.M., Ishman, S.E., Poore, R.Z., Willard, D.A. and Holtz Jr., T.R., 1993. Paleoclimatic reconstructions of a warmer Earth: PRISM Middle Pliocene Northern Hemisphere synthesis. Global Planet. Change, 9: 169–195.

Hansen, J.E., Fung, I., Lacis, A., Rind, D., Lebedeff, S., Ruedy, R. and Russell, G., 1988. Global climate changes as forecast by Goddard Institute for Space Studies three-dimensional model. J. Geophys. Res., 93: 9341–9364.

Hansen, J.E., Lacis, A., Rind, D., Russell, G., Stone, P., Fung, I., Ruedy, F. and Lerner, J., 1984. Climate sensitivity: Analysis of feedback mechanisms. In: J.E. Hansen and T. Takahashi (Editor), Climate Processes and Climate Sensitivity. Am. Geophys. Union, Washington, DC, pp. 130–163.

Hansen, J.E., Lacis, A., Ruedy, R., Sato, M. and Wilson, H., 1993. How sensitive is the world's climate? Res. Explor., 9: 142–158.

Hansen, J.E., Russell, G., Rind, D., Stone, P., Lacis, A., Lebedeff, S., Ruedy, R. and Travis, L., 1983. Efficient three-dimensional global models for climate studies: Models I and II. Mon. Weather Rev., 111: 609–662.

Haq, B.H., Hardenbol, J. and Vail, P.R., 1987. Chronology of fluctuating sea levels since the Triassic. Science, 235: 1156–1167.

Harwood, P.J., 1986. Diatom biostratigraphy and paleoecology with a Cenozoic history of Antarctic ice sheets. Thesis. Ohio State Univ., Columbus, Ohio, 592 pp.

Hoffert, M.I. and Covey, C., 1992. Deriving global climate sensitivity from paleoclimate reconstructions. Nature, 360: 573–576.

Hostetler, S.W., Giorgi, F., Bates, G.T. and Bartlein, P.J., 1994. Lake–atmosphere feedbacks associated with paleolakes Bonneville and Lahontan. Science, 263: 665–667.

Kutzbach, J.E. and Guetter, P.J., 1986. The influence of changing orbital parameters and surface boundary conditions on climate simulations for the past 18 000 years. J. Atmos. Sci., 43: 1726–1759.

Maier-Reimer, E., Mikolajewicz, U. and Crowley, T.J., 1990. Ocean general circulation model sensitivity experiment with an open Central American isthmus. Paleoceanography, 5: 349–366.

Manabe, S. and Broccoli, A.J., 1985. The influence of continental ice sheets on the climate of an ice age. J. Geophys. Res., 90: 2167–2190.

Matthews, E., 1984. Prescription of land-surface boundary conditions in GISS GCM II: A simple method based on high-resolution vegetation data bases. NASA Techn. Mem., 86096, NASA Goddard Space Flight Center Inst. Space Stud., p. 20.

Miller, J.R., Russell, G.L. and Lie-Ching, T., 1983. Annual oceanic heat transports computed from an atmospheric model. Dyn. Atmos. Oceans, 7: 95–109.

Molnar, P. and England, P., 1990. Late Cenozoic uplift of mountain ranges and global climate change: chicken or egg? Nature, 346: 29–34.

Molnar, P., England, P. and Martinod, J., 1993. Mantle dynamics, uplift of the Tibetan Plateau, and the Indian monsoon. Rev. Geophys., 31: 357–396.

Moore, G.T., Hayashida, D.N., Ross, C.A. and Jacobson, S.R., 1992. Paleoclimate of the Kimmeridgian/Tithonian (Late Jurassic) world: 1. Results using a general circulation model. Palaeogeogr., Palaeoclimatol., Palaeoecol., 93: 113–150.

Ramanathan, V., Barkstrom, B.R. and Harrison, E.F., 1989. Climate and the Earth's radiation budget. Phys. Today, 42: 22–32.

Raymo, M.E. and Rau, G., 1992. Plio-Pleistocene atmospheric CO_2 levels inferred from POM $\delta^{13}C$ at DSDP Site 607 (Abstract). Eos, Trans. Am. Geophys. Union, Suppl., 73, p. 95.

Raymo, M.E. and Ruddiman, W.F., 1992. Tectonic forcing of late Cenozoic climate. Nature, 359: 117–122.

Raymo, M.E., Ruddiman, W.F. and Froelich, P.N., 1988. Influence of Late Cenozoic mountain building on ocean geochemical cycles. Geology, 16: 649–653.

Rind, D., 1986. The dynamics of warm and cold climates. J. Atmos. Sci., 43: 3–24.

Rind, D., 1987a. Components of the Ice Age circulation. J. Geophys. Res., 92: 4241–4281.

Rind, D., 1987b. The doubled CO_2 climate: Impact of the sea surface temperature gradient. J. Atmos. Sci., 44: 3235–3268.

Rind, D., 1988. The doubled CO_2 climate and the sensitivity of the modelled hydrologic cycle. J. Geophys. Res., 93: 5385–5412.

Rind, D., 1992. An uplifting experience. Nature, 360: 414–415.

Rind, D. and Chandler, M.A., 1991. Increased ocean heat transports and warmer climate. J. Geophys. Res., 96: 7437–7461.

Ruddiman, W.F. and Kutzbach, J.E., 1989. Forcing of Late Cenozoic Northern Hemisphere climate by plateau uplift in southeast Asia and the American southwest. J. Geophys. Res., 94: 18,409–18,428.

Russell, G., Miller, J.R. and Tsang, L.-C., 1985. Seasonal oceanic heat transports computed from an atmospheric model. Dyn. Atmos. Oceans, 9: 253–271.

Schneider, S.H., Thompson, S.L. and Barron, E.J., 1985. Mid-Cretaceous continental surface temperatures: Are high CO_2 concentrations needed to simulate above-freezing winter conditions? In: E.T. Sundquist and W.S. Broecker (Editors), The Carbon Cycle and Atmospheric CO_2: Archean to Present (Geophys. Monogr., 32). Am. Geophys. Union, Washington, DC, pp. 554–560.

Sloan, L.C. and Barron, E.J., 1990. "Equable" climates during Earth history? Geology, 18: 489–492.

Sloan, L.C. and Barron, E.J., 1992. A comparison of Eocene climate model results to quantified paleoclimatic interpretations. Palaeogeogr., Palaeoclimatol., Palaeoecol., 93: 183–202.

Tselioudis, G., Rossow, W.B. and Rind, D., 1992. Global pattern of cloud optical thickness variation with temperature. J. Climate, 5: 1484–1495.

Tselioudis, G., Lacis, A.A., Rind, D. and Rossow, W.B., 1993. Potential effects of cloud optical thickness on climate. Nature, 366: 670–672.

Valdes, P.J. and Sellwood, B.W., 1992. A palaeoclimate model for the Kimmeridgian. Palaeogeogr., Palaeoclimatol., Palaeoecol., 95: 47–72.

Wallace, J.M. and Hobbs, P.V., 1977. Atmospheric Science: An Introductory Survey. Academic Press, Orlando, 467 pp.